Submitted to Geophysics

LBL-10649
Preprint

A SOLUTION FOR TM-MODE PLANE WAVES INCIDENT ON A TWO-DIMENSIONAL INHOMOGENEITY

K. H. Lee and H. F. Morrison

March 1980

Prepared for the U.S. Department of Energy
under Contract W-7405-ENG-48

DISCLAIMER

A SOLUTION FOR TM-MODE PLANE WAVES INCIDENT ON A TWO-DIMENSIONAL INHOMOGENEITY

K. H. Lee and H. F. Morrison

Lawrence Berkeley Laboratory
Engineering Geoscience
University of California
Berkeley, CA 94720

ABSTRACT

A solution for the electromagnetic fields scattered from a two-dimensional inhomogeneity in a conducting half space has been obtained for an incident TM mode plane wave; the magnetic field is polarized parallel to the strike of the inhomogeneity. The approach has been to determine the scattering currents within the inhomogeneity using an integral equation for the electric fields. This solution is similar in concept to earlier studies of TE mode scattering from two-dimensional inhomogeneities, and it completes the analysis of the scattering of arbitrary plane waves using the integral equation approach. For simple bodies in the earth integral equation solution offers significant computational advantages over alternate finite element or finite difference methods of solution.

Introduction

Quantitative interpretation of magnetotelluric surveys depends at present on the availability of efficient forward modeling algorithm. To date two major numerical techniques have been used to obtain the scattered fields from buried inhomogeneities in plane wave fields; methods solving the governing differential equation which generally uses a finite element or finite difference approach and methods which solve an integral equation formulation of the problem.

For two-dimensional inhomogeneities a solution for incident fields with the electric field parallel to the strike of the inhomogeneity (TE mode solution) has been developed by Hohmann (1970) using the integral equation approach. For a perfect conductor an integral formulation, for surface scattering currents, for the TM mode (magnetic field parallel to the strike of the inhomogeneity) has been developed by Parry (1969). General two-dimensional solutions in the presence of an arbitrary mode plane wave (mixed TE-TM) have been obtained by Ryu (1971), Swift (1971), and Rijo (1977) using either a finite element or finite difference technique.

To our knowledge the TM integral equation solution for the general case has not been presented. The solution presented here thus completes the analysis for the scattering of arbitrary mode plane waves from two-dimensional inhomogeneities using the integral equation approach. Apart from significant computational advantages in forward modeling of simple geologic bodies for magnetotelluric analysis, this solution is important for evaluating the results of alternate numerical methods used for more complicated geologic models. It is becoming evident that for many of

the current numerical modeling schemes, there are no convincing checks on the accuracy of the solution. It is imperative therefore that several solutions be obtained by differing methods and be compared until confidence is attained in these solutions.

1. Formulation of two-dimensional integral equations

In their general form, Maxwell's equations are written as follows:

$$-\nabla\times\bar{E} = j\omega\mu\bar{H} + \bar{M}^{i} \tag{1.1}$$

$$\nabla\times\bar{H} = (\sigma + j\omega\varepsilon)\,\bar{E} + \bar{J}^{i} \tag{1.2}$$

where $\bar{M}^{i}$ and $\bar{J}^{i}$ are impressed magnetic and electric currents. Throughout the paper an $e^{j\omega t}$ time dependence is assumed. Harrington (1961) has shown that a generalized integral equation solution can be obtained by rewriting (1.1) and (1.2) as

$$-\nabla\times\bar{E} = j\omega\mu_1\bar{H} + \bar{M}^{s} + \bar{M}^{i} \tag{1.3}$$

$$\nabla\times\bar{H} = (\sigma_1 + j\omega\varepsilon_1)\,\bar{E} + \bar{J}^{s} + \bar{J}^{i} \tag{1.4}$$

where $\bar{M}^{s}$ and $\bar{J}^{s}$ are scattering magnetic and electric currents representing the inhomogeneities in the half space of electric and magnetic constants σ_1, μ_1, and ε_1 (Figure 1.1). Equating the right hand sides of (1.1) and (1.2) to those of (1.3) and (1.4) respectively, we find that the scattering currents are zero everywhere except for the inhomogeneous region, in which

$$\bar{M}^{s} = j\omega(\mu_2 - \mu_1)\,\bar{H} \tag{1.5.1}$$

$$\bar{J}^S = \Delta\sigma\bar{E} \qquad (1.5.2)$$

where

$$\Delta\sigma = (\sigma_2 - \sigma_1) + j\omega(\varepsilon_2 - \varepsilon_1) \ .$$

In the absence of active sources and magnetic inhomogeneities, equations (1.3) and (1.4) become

$$-\nabla\times\bar{E} = j\omega\mu_1\bar{H} \qquad (1.6)$$

$$\nabla\times\bar{H} = (\sigma_1 + j\omega\varepsilon_1)\,\bar{E} + \bar{J}^S \ . \qquad (1.7)$$

The total field can always be written as the sum of the incident (i) field, the field that would exist in the absence of the inhomogeneity, and the scattered field (s), such that

$$\bar{E} = \bar{E}^i + \bar{E}^S \qquad (1.8)$$

$$\bar{H} = \bar{H}^i + \bar{H}^S \ , \qquad (1.9)$$

and consequently Maxwell's equations for the scattered fields are written as

$$-\nabla\times\bar{E}^S = j\omega\mu_1\bar{H}^S \qquad (1.10)$$

$$\nabla\times\bar{H}^S = (\sigma_1 + j\omega\varepsilon_1)\,\bar{E}^S + \bar{J}^S \ . \qquad (1.11)$$

Equations (1.10) and (1.11) lead to a Helmholtz equation for the scattered field $\bar{E}^s$ in the inhomogeneous region

$$\left(\nabla^2 + k_1^2\right) \bar{E}^s = j\omega\mu_1 \bar{J}^s \quad . \tag{1.12}$$

The solution for (1.12) can generally be written in the form of an integral equation as

$$\bar{E}^s(\bar{r}) = \iint_{s'} \bar{\bar{G}}^E(\bar{r};\bar{r}') \cdot \bar{J}^s(\bar{r}') \, ds \tag{1.13}$$

and

$$\bar{H}^s(\bar{r}) = \iint_{s'} \bar{\bar{G}}^H(\bar{r};\bar{r}') \cdot \bar{J}^s(\bar{r}') \, ds \tag{1.14}$$

where $\bar{r}$ and $\bar{r}'$ are the vectors describing the positions of observation and source respectively. $\bar{\bar{G}}(\bar{r};\, \bar{r}')$ is a two-dimensional Green's tensor defined as the scattered field at $\bar{r}$ caused by a unit current density located at $\bar{r}'$.

One way of obtaining $\bar{\bar{G}}(\bar{r};\bar{r}')$ is to find a single vector potential $\bar{\pi}$ and relate it to the scattered fields defined by

$$\bar{E}^s = k^2\bar{\pi} + \nabla(\nabla \cdot \bar{\pi}) \tag{1.15}$$

$$\bar{H}^s = (\sigma + j\omega\varepsilon) \, \nabla \times \bar{\pi} \tag{1.16}$$

where $\bar{\pi}$ is the electric Hertz vector satisfying the inhomogeneous Helmholtz equation.

$$(\nabla^2 + k^2)\ \bar{\pi} = -\frac{\bar{J}^s}{\sigma + j\omega\varepsilon}\ \delta(x - x')\ \delta(z - z') \qquad (1.17)$$

in Cartesian coordinates. The particular solution for (1.17) is shown in Appendix A as

$$\bar{\pi}^p = -\frac{j\omega\mu}{2\pi}\frac{\bar{J}^s}{k^2}\int_0^\infty \frac{1}{u}\, e^{-u|z-z'|}\cos kx(x-x')\ dk_x \qquad (1.18)$$

where

$$u = \left(k_x^{\,2} - k^2\right)^{1/2} .$$

The homogeneous solution $\bar{\pi}^s$ for (1.17) is subject to the boundary conditions and it satisfies

$$(\nabla^2 + k^2)\ \bar{\pi}^s = 0 . \qquad (1.19)$$

The total vector potentials in the homogeneous half space generated by current elements in it are given by Appendix A.

$$\pi_{1x} = -\frac{j\omega\mu}{2}\frac{J_x}{k_1^2}\int_0^\infty \frac{1}{u_1}\left[e^{-u_1|z-z'|} + R_{TM}e^{-u_1(z+z')}\right]\cos k_x(x-x')\ dk_x \qquad (1.20)$$

$$\pi_{1z} = -\frac{j\omega\mu}{2\pi}\frac{J_z}{k_1^2}\int_0^\infty \frac{1}{u_1}\left[e^{-u_1|z-z'|} - R_{TM}e^{-u_1(z+z')}\right]\cos k_x(x-x')\ dk_x \qquad (1.21)$$

where

$$R_{TM} = -\frac{k_0^2 u_1 - k_1^2 u_0}{k_0^2 u_1 + k_1^2 u_0}$$

and J_x and J_z are the scattering current densities directed in x and z respectively.

From equations (1.15) and (1.16) and by the definition of Green's function, the elements of Green's tensors $\bar{\bar{G}}^E(\bar{r};\bar{r}')$ and $\bar{\bar{G}}^H(\bar{r};\bar{r}')$ can be written as

$$G^E_{xx} = \left(k_1^2 + \frac{\partial^2}{\partial x^2}\right)\pi'_{1x} \tag{1.22}$$

$$G^E_{zx} = \frac{\partial^2}{\partial z \partial x}\pi'_{1x} \tag{1.23}$$

$$G^H_{yx} = -\frac{k_1^2}{j\omega\mu}\frac{\partial}{\partial z}\pi'_{1x} \tag{1.24}$$

$$G^E_{xz} = \frac{\partial^2}{\partial x \partial z}\pi'_{1z} \tag{1.25}$$

$$G^E_{zz} = \left(k_1^2 + \frac{\partial^2}{\partial z^2}\right)\pi'_{1z} \tag{1.26}$$

$$G^H_{yz} = \frac{k_1^2}{j\omega\mu}\frac{\partial}{\partial x}\pi'_{1z} \tag{1.27}$$

where the primed potentials π'_{1x} and π'_{1z} are just the potentials due to a unit current densities of J_x and J_z respectively. One can easily verify the reciprocity theorem by substituting (1.20) and (1.21) through (1.27).

With $\bar{\bar{G}}^E(\bar{r};\bar{r}')$ and $\bar{\bar{G}}^H(\bar{r};\bar{r}')$ known, the total fields at $\bar{r}$ can be rewritten for (1.8) and (1.9) as

$$\bar{E}(\bar{r}) = \bar{E}^i(\bar{r}) + \iint_{S'} \bar{\bar{G}}^E(\bar{r};\bar{r}') \cdot \bar{J}^s(\bar{r}')\, ds \tag{1.28}$$

$$\bar{H}(\bar{r}) = \bar{H}^i(\bar{r}) + \iint_{S'} \bar{\bar{G}}^H(\bar{r};\bar{r}') \cdot \bar{J}^s(\bar{r}')\, ds \quad . \tag{1.29}$$

2. Evaluation of the integral equation

Computation of the scattering current

It is the definition of the scattering current $\bar{J}^S$ that enables us to compute the electric field $\bar{E}$ in the inhomogeneity. In other words, upon substituting equation (1.5.2) into integral equation (1.28), we can solve for the electric field in the inhomogeneous region provided that the Green's function and the incident field are known. In practice the inhomogeneous region, S', is divided into a finite number of rectangular cells, Figure 2.1, such that a constant current density over each call can be assumed. With this assumption the integral equation (1.28) can be rewritten as

$$\bar{E}_i = \bar{E}^i_i + \sum_{j=1}^{N} \Delta\sigma_j \left(\bar{\bar{\Gamma}}^E_{ij} \cdot \bar{E}_j \right), \quad i = 1,N \tag{2.1}$$

where

$$\bar{\bar{\Gamma}}^E_{ij} = \begin{pmatrix} \Gamma^E_{xxij} & \Gamma^E_{xzij} \\ \Gamma^E_{zxij} & \Gamma^E_{zzij} \end{pmatrix} . \tag{2.2}$$

The elements composing $\bar{\bar{\Gamma}}^E_{ij}$ are integrated Green's functions, for example,

$$\Gamma^E_{zxij} = \iint_{S'_j} G^E_{zx}(\bar{r}_i;\bar{r}') \, ds \tag{2.3}$$

where the integration is carried out over the j^{th} cell of S'.

Using the quasistatic approximation, $k_0 \sim 0$, we can reduce the factor R_{TM} to

$$R_{TM} = 1, \qquad \text{for all } k_x . \tag{2.4}$$

It can be shown that the integrations in K_x space leads to the following analytic results for π'_{1x} and π'_{1z}

$$\pi'_{1x} = - \frac{j\omega\mu}{z\pi} \frac{1}{k_1^2} \left[K_0(jk_1 r_1) + K_0(jk_1 r_2) \right] \tag{2.5}$$

$$\pi'_{1z} = - \frac{j\omega\mu}{z\pi} \frac{1}{k_1^2} \left[K_0(jk_1 r_1) - K_0(jk_1 r_2) \right] \tag{2.6}$$

where K_0 is the modified Bessel function of the second kind of order zero, and

$$r_1 = \left[(x - x')^2 + (z - z')^2 \right]^{1/2} .$$

$$r_2 = \left[(x - x')^2 + (z + z')^2 \right]^{1/2}$$

The evaluation of $\overline{\overline{\Gamma}}$ is given by Appendix B. Special care is taken for the situation where the Green's function becomes singular. Rewriting the results for the electric fields,

$$\Gamma^E_{xxij} = \frac{j\omega\mu}{k_1^2} S_{ij} - \frac{\omega\mu}{2\pi k_1} \int_{x_\ell}^{x_r} \left[\frac{z_i - z'}{r_1} K_1(jk_1 r_1) - \frac{z_i + z'}{r_2} K_1(jk_1 r_2) \right] \Bigg|_{z_t}^{z_b} dx' \tag{2.7}$$

$$\Gamma^E_{zxij} = - \frac{j\omega\mu}{2\pi} \frac{1}{k_1^2} \left[K_0(jk_1 r_1) - K_0(jk_1 r_2) \right] \Bigg|_{x_\ell}^{x_r} \Bigg|_{z_t}^{z_b} \tag{2.8}$$

$$\Gamma^{E}_{xzij} = -\frac{j\omega\mu}{2\pi}\frac{1}{k_1^2}\left[K_0(jk_1r_1) + K_0(jk_1r_2)\right]\Bigg|_{x_\ell}^{x_r}\Bigg|_{z_t}^{z_b} \tag{2.9}$$

$$\Gamma^{E}_{zzij} = \frac{j\omega\mu}{k_1^2}S_{ij} - \frac{\omega\mu}{2\pi k_1}\int_{z_t}^{z_b}\left[\frac{x_i-x'}{r_1}K_1(jk_1r_1) - \frac{x_i-x'}{r_2}K_1(jk_1r_2)\right]\Bigg|_{x_\ell}^{x_r}dz' \tag{2.10}$$

where

$$S_{ij} = 1, \quad \text{for } x_\ell < x_i < x_r \text{ and } z_t < z_i < z_b$$

$$S_{ij} = 0, \quad \text{for } (x_i, z_i) \text{ outside of } s'_j$$

and

$$f(t)\Big|_{t_1}^{t_2} = f(t_2) - f(t_1) . \tag{2.11}$$

The notations x_ℓ, x_r, z_t, and z_b are shown in Figure 2.1, and they are consistent with those used in Appendix B.

Equation (2.1) can now be rewritten in a numerically equivalent matrix form as

$$\bar{\bar{K}} \cdot \bar{E} = -\bar{E}^i \tag{2.12}$$

where the elements of K are given by

$$\bar{\bar{K}}_{ij} = \Delta\sigma_j \bar{\bar{\Gamma}}^{E}_{ij} - \bar{\bar{\delta}}_{ij}, \qquad i,j = 1,N$$

with

$$\bar{\bar{\delta}}_{ij} = \begin{pmatrix} 1 & 0 \\ 0 & 1 \end{pmatrix}, \qquad \text{for} \quad i = j$$

and

$$\bar{\bar{\delta}}_{ij} = \begin{pmatrix} 0 & 0 \\ 0 & 0 \end{pmatrix}, \qquad \text{for} \quad i \neq j \ .$$

The electric field in the body is found by

$$\bar{E} = - \bar{\bar{K}}^{-1} \cdot \bar{E}^{i} \tag{2.13}$$

where the incident field $\bar{E}^{i}$ can be easily computed in the absence of the inhomogeneity. The scattering current $\bar{J}^{s}$ is then simply given by equation (1.5.2).

Computation of the fields on the surface

The electric and magnetic fields outside of the body are obtained using the same integral equations (1.28) and (1.29) by substituting the scattering current obtained in the foregoing section. The Green's function is evaluated at the earth's surface. Equation (2.1) is slightly modified to

$$\bar{E}_k \Big|_{z_k=0} = \bar{E}^{i} \Big|_{z_{k=0}} + \sum_{j=1}^{N} \bar{\bar{\Gamma}}^{E}_{kj} \Big|_{z_k=0} \cdot \bar{J}^{s} \tag{2.14}$$

and for the magnetic field

$$\bar{H}_k\Big|_{z_k=0} = \bar{H}^i\Big|_{z_k=0} + \sum_{j=1}^{N} \bar{\bar{\Gamma}}^H_{kj}\Big|_{z_k=0} \cdot \bar{J}^s, \qquad k = 1,M \tag{2.15}$$

where

$$\bar{\bar{\Gamma}}^E_{kj}\Big|_{z_k=0} = \begin{pmatrix} \Gamma^E_{xxkj} & \Gamma^E_{xzkj} \\ \Gamma^E_{zxkj} & \Gamma^E_{zzkj} \end{pmatrix}_{z_k=0} \tag{2.16}$$

$$\bar{\bar{\Gamma}}^H_{kj}\Big|_{z_k=0} = \begin{pmatrix} \Gamma^H_{yxkj} & \Gamma^H_{yzkj} \end{pmatrix}_{z_k=0} \tag{2.17}$$

and M is the number of field points on the surface.

It can be shown that the integrated Green's functions evaluated at the surface are as follows;

$$\Gamma^E_{xxkj}\Big|_{z_k=0} = \frac{\omega\mu}{\pi k_1} \int_{x_\ell}^{x_r} \left[\frac{z'}{r_0} K_1(jk_1r_0)\right] \Big|_{z_t}^{z_b} dx' \tag{2.18.1}$$

for $z_t > 0$, and

$$\Gamma^E_{xxkj}\Big|_{z_k=0} = \frac{j\omega\mu}{k_1^2} + \frac{\omega\mu}{\pi k_1} \int_{x_\ell}^{x_r} \left[\frac{z'}{r_0} K_1(jk_1r_0)\right]_{z_b} dx' \tag{2.18.2}$$

for $z_t = 0$ and $x_r < x_k < x_\ell$.

$$\Gamma^E_{xzkj}\Big|_{z_k=0} = -\frac{j\omega\mu}{\pi} \frac{1}{k_1^2} K_0(jk_1r_0) \Big|_{x_\ell}^{x_r} \Big|_{z_t}^{z_b} \tag{2.19}$$

with r_o in (2.18.1), (2.18.2), and (2.19) defined as

$$r_o = \left[(x_k - x')^2 + z'^2\right]^{1/2}$$

It should be noticed that

$$\Gamma^{E}_{zxkj}\Big|_{z_k=0} = \Gamma^{E}_{zzkj}\Big|_{z_j=0} = \Gamma^{H}_{yxkj}\Big|_{z_k=0} = \Gamma^{H}_{yzkj}\Big|_{z_k=0} = 0 \ . \tag{2.20}$$

In other words, there is no secondary vertical(z) electric field or horizontal(y) magnetic field caused by the scatterer in the half space.

3. Scattering in a two-layered earth

Consider the case of a conductive body buried in the lower half space of a two-layered earth. The vector potentials in the first and second layers are found in Appendix A. Rewriting the results by making use of the quasistatic approximation, $k_0 \sim 0$,

$$\pi'_{1x} = -\frac{j\omega\mu}{2\pi}\frac{1}{k_1^2}\int_0^\infty \frac{u_2}{u_1^2}\,{}^1R_{TM}\cdot\left(e^{u_1 z}+e^{-u_1 z}\right)e^{-u_2 z'}\cos k_x(x-x')dk_x \tag{3.1}$$

$$\pi'_{1z} = -\frac{j\omega\mu}{2\pi}\frac{1}{k_1^2}\int_0^\infty \frac{1}{u_1}\,{}^1R_{TM}\cdot\left(e^{u_1 z}-e^{-u_1 z}\right)e^{-u_2 z'}\cos k_x(x-x')dk_x \tag{3.2}$$

$$\pi'_{2x} = -\frac{j\omega\mu}{2\pi}\frac{1}{k_2^2}\left[K_0(jk_2 r)+\int_0^\infty \frac{1}{u_2}\,{}^2R_{TM}\cdot e^{-u_2(z+z'-2d)}\cos k_x(x-x')\,dk_x\right] \tag{3.3}$$

$$\pi'_{2z} = -\frac{j\omega\mu}{2\pi}\frac{1}{k_2^2}\left[K_0(jk_2 r)-\int_0^\infty \frac{1}{u_2}\,{}^2R_{TM}\cdot e^{-u_2(z+z'-2d)}\cos kx(x-x')\,dx_x\right] \tag{3.4}$$

where

$$ {}^{1}R_{TM} = \frac{e^{u_2 d}\ \text{sech}\ u_1 d}{\left(\frac{k_2}{k_1}\right)^2 + \frac{u_2}{u_1}\tanh u_1 d} $$

$$ {}^{2}R_{TM} = \frac{\left(\frac{k_2}{k_1}\right)^2 - \frac{u_2}{u_1}\tanh u_1 d}{\left(\frac{k_2}{k_1}\right)^2 + \frac{u_2}{u_1}\tanh u_1 d} $$

and d is the thickness of the first layer. The Green's function in each layer is given by equations (1.22) through (1.27). The scattering currents are computed by using π'_{2x} and π'_{2z} in the lower half space in the usual manner discussed in the homogeneous half space case.

The scattering currents in the lower half space

The integrated Green's functions to be used for the formulation of equation (2.1) are found in Appendix C as

$$ \Gamma^{E}_{xxij} = \frac{j\omega\mu}{k_2^2} S_{ij} - \frac{\omega\mu}{2\pi k_2} \int_{x_\ell}^{x_r} \left[\frac{z_i - z'}{r} K_1(jk_2 r)\right] \Big|_{z_t}^{z_b} dx' $$

$$ + \frac{j\omega\mu}{2\pi}\frac{1}{k_2^2} \int_0^\infty {}^{2}R_{TM}\, e^{-u_2 z_i} \left[e^{-u_2 z'} \sin k_x(x_i - x')\right] \Big|_{x_\ell}^{x_r} \Big|_{z_t}^{z_b} dk_x \qquad (3.5) $$

$$ \Gamma^{E}_{yxij} = -\frac{j\omega\mu}{2\pi}\frac{1}{k_2^2} K_0(jk_2 r) \Big|_{x_\ell}^{x_r} \Big|_{z_t}^{z_b} $$

$$ + \frac{j\omega\mu}{2\pi}\frac{1}{k_2^2} \int_0^\infty \frac{{}^{2}R_{TM}}{u_2} e^{-u_2 z_i} \left[e^{-u_2 z'} \cos k_x(x_i - x')\right] \Big|_{x_\ell}^{x_r} \Big|_{z_t}^{z_b} dk_x \qquad (3.6) $$

$$\Gamma^{E}_{xzij} = -\frac{j\omega\mu}{2\pi}\frac{1}{k_2^2}K_0(jk_2r)\Big|_{x_\ell}^{x_r}\Big|_{z_t}^{z_b} - \frac{j\omega\mu}{2\pi}\frac{1}{k_2^2}\int_0^\infty \frac{2R_{TM}}{u_2}e^{-u_2z_i}\left[e^{-u_2z'}\cos k_x(x_i-x')\right]\Big|_{x_\ell}^{x_r}\Big|_{z_t}^{z_b}dk_x \tag{3.7}$$

$$\Gamma^{E}_{zzij} = \frac{j\omega\mu}{k_2^2}S_{ij} - \frac{\omega\mu}{2\pi k_2}\int_{z_t}^{z_b}\left[\frac{x_i-x'}{r}K_1(jk_2r)\right]\Big|_{x_\ell}^{x_r}dz' + \frac{j\omega\mu}{2\pi}\frac{1}{k_2^2}\int_0^\infty \frac{k_x^2}{u_2^2}R_{TM}e^{-u_2z_i}\left[e^{-u_2z'}\sin k_x(x_i-x')\right]\Big|_{x_\ell}^{x_r}\Big|_{z_t}^{z_b}dk_x \tag{3.8}$$

Once the elements of Green's tensor are computed, the electric fields in the body are found by (2.13) and finally the scattering currents are computed by (1.5.2). These elements can not, in this case, be integrated analytically and consequently extremely time consuming numerical integration in k_x must be carried out.

Computation of the fields on the surface

The electric and magnetic fields are computed in the usual manner. However, the Green's function to be used for the surface fields differs from that used in the lower half space. The elements of integrated Green's tensors evaluated at the k^{th} field point (x_k, $z_k = 0$) are given by Appendix B.

(3.9)

$$\Gamma^{E}_{xzkj}\Big|_{z_k=0} = -\frac{j\omega\mu}{\pi}\frac{1}{k_1^2}\int_0^{\infty}\frac{1}{u_2}R_{TM}\left[e^{-u_2 z'}\cos k_x(x_k-x')\right]\Big|_{x_\ell}^{x_r}\Big|_{z_t}^{z_b} dk_x \tag{3.10}$$

$$\Gamma^{H}_{yxkj}\Big|_{z_k=0} = \Gamma^{H}_{yzkj}\Big|_{z_k=0} = \Gamma^{E}_{zxkj}\Big|_{z_k=0} = \Gamma^{E}_{zzkj}\Big|_{z_k=0} = 0. \tag{3.11}$$

Substituting these elements into equations (2.14) and (2.15), we obtain the total electric and magnetic fields on the surface. It is interesting to notice that, on the surface of the earth, neither the horizontal secondary magnetic field (H_y^s) nor the vertical electric field (E_z^s) is present. The same result was obtained for the homogeneous half space.

4. Computation and evaluation of the results

There are basically two kinds of numerical integrations involved in the previous sections. They may be symbolically represented by:

$$I_1 = \int_{x_1}^{x_2} f_1(x)\,dx \tag{4.1}$$

$$I_2 = \int_0^{\infty} f_2(x)\begin{pmatrix}\sin ax\\ \cos ax\end{pmatrix}dx\ . \tag{4.2}$$

The first integration can be done by simply discretizing the short

interval into a proper number of small sections Δx_i , such that

$$I_1 \doteq \sum_{i=1}^{p} f(x_i)\, \Delta x_i \ . \tag{4.3}$$

The operation is simple and fast. The number p is kept to a minimum because the integrand $f_1(x)$ is a slowly varying function of x in the interval specified. The second type of integration is rather time consuming, especially when $|a|$ is large so that the functional fluctuates more rapidly. Since the major contribution to I_2 comes from the first few cycles of the trigonometric function used, we may approximate I_2 as

$$I_2 \doteq \sum_{i=1}^{g} \int_{x_{i-1}}^{x_i} f_2(x) \begin{pmatrix} \sin ax \\ \cos ax \end{pmatrix} dx \tag{4.4}$$

where g is the number of half cycles. Each half cycle is evaluated by a Gaussian quadrature routine. The number g is increased until a given convergence criterion is met.

The numerical results obtained here have been compared to the solutions found by Ryu (1970) using the finite element method. Apparent resistivity and the phase of impedance are derived accordingly from both solutions.

The first model is a rectangular conductor of 200m x 50m in size buried in a homogeneous half space with varying depths to the top of the conductor. Figure 4.1 and Figure 4.2 illustrate the responses of the same conductor exposed to the incident fields of 100 Hz and 8 Hz

respectively. The heavy and dotted lines represent the apparent resistivities and the impedance phases respectively. The symbols ◇ and * denote the corresponding solutions obtained using the finite element method. Within the range of $\pm$ 0.5 km, both methods generate basically the same solutions except for the minor disagreements displayed at the top of the center of the body. However, as the depth to the top of the conductor decreases, the gaps between two solutions become significant at the center, especially when the comparison is made for the phase of impedance.

It has been observed that the finite element solution, aided by a recently developed fast matrix inversion routine, needs more than twice the computing time required for the integral equation solution for this particular model. Explicitly, it takes 3 seconds by CDC 7600 to obtain one integral equation solution, for which the given model is broken into 16 small square cells.

The next model investigated is a conductive dyke with varying angles of dip as is shown by Figure 4.3. A dipping boundary of the body is simulated by stacking small rectangular conductors in such a way that the overall dip angle is preserved.

A maximum phase difference of 5^{0} is observed between the models for $\alpha = 0^{0}$ and $\alpha = 45^{0}$. In the down dip direction for the case of $\alpha = 45^{0}$, the apparent resistivities obtained from the integral equation solution are up to 25% higher than in the solutions obtained by using finite element method. The main reason for this is that the cell size chosen here, 25m x 25m, is not small enough for either method; 25m is only half the skin depth in the body for the frequency used. Because of the dipolar characteristics of the electric fields, the surface fields are strongly

dominated by those current elements close to the surface. In other words, small errors associated with the scattering currents in the cells close to the surface could cause significant effects on the surface fields. The effects are relatively stronger where the true magnitudes of the electric fields are smaller.

Figure 4.4 shows the anomalies of the same conductor used in the first model with an overburden of 25m in thickness. The resistivity of the top layer plays a major role in determining the background apparent resistivity as well as the phase of the impedence. With three different resistivities of 5, 10, and 25 ohm-m assigned to the top layer, the phase anomaly never exceeds 5 degrees and there is only a small, constant, phase difference between the two techniques. As far as the effects of the overburden and the medium surrounding the body are concerned, they are analytically taken into account by the integral equation through the Green's function. Therefore, the small differences in apparent resistivity between the two solutions is likely due to the finite element solution where the same kind of linear field behavior is imposed upon the elements within the body as well as outside of the body including the overburden.

5. Remarks

The solution of the integral equation depends primarily on finding a Green's function pertinent to the geometry under investigation. It is unfortunate that the available Green's functions are limited to those for layered half spaces. However, given the Green's functions, it is necessary to solve for the scattering current only in the inhomogeneous region. This is the major advantage of the method discussed here over the finite difference techniques.

Because of the complexity involved in finding the Green's function, half spaces composed of more than two layers have not been considered. Major emphasis has been given to the case where the earth is a homogeneous half space. In this case, both primary and secondary Green's functions have been shown to be analytic. Hence, the integral equation approach is better than the finite difference technique for simple inhomogeneities such as a thin dyke or some other small conductors buried in a homogeneous half space.

The following chart illustrates the comparisons between the two methods in terms of the total computing units, and the costs, required for the computations of the fields for a single frequency.

	Finite Element		Integral Equation	
	CPU	Cost ($)	CPU	(Cost ($)
Model 1	40.	1.70	7.	.50
Model 2	165.	11.	15.	1.10
Model 3	45	1.80	40.	2.20

The Lawrence Berkeley Laboratory CDC 7600 computer has been used for the computations. We have selected 34 surface field positions (17 for the symmetric bodies) for apparent resistivity profiles drawn in the Figures.

The series expansions of the modified Bessel functions, K_0 and K_1, and the numerical integrations in k_x space converge faster when $|\bar{r}-\bar{r}'|$ is small. It has been observed that approximately two thirds of the total computing time is spent for the computations of the surface fields for the models considered here.

A remarkable advantage of the integral equation approach can be

found in a magnetotelluric study. Suppose we wish to have the response at 30 frequencies at one station on the surface of Model 1. The cost required for the computations of the electric fields in the body for 30 frequencies will be \$5, a third of 50 cents multiplied by 30. Since the average cost required for the computation of a surface field will be two thirds of 50 cents divided by 17 field positions, it will cost less than \$1 for 30 frequencies at a single location. The total cost required for the computation of the response at one magnetotelluric station will be \$6 by the method discussed here compared to approximately \$50 (30 frequencies multiplied by \$1.70) by the finite element method. The two methods become effectively the same in terms of computing costs for a model, the inhomogeneous cross sectional area of which is approximately 10 squared skin depths, a size equivalent to 40 square cells of .5 x .5 skin depths.

Another advantage of the integral equation approach is that it offers an easy access to the derivatives of the field quantities, a procedure necessary for the inversion of the field data.

Rewriting equation (2.1) with $\Delta\sigma_j$ substituted by $(\sigma_j-\sigma)$ in the expression:

$$\vec{E}_i = \vec{E}_i^1 + \sum_{j=1}^{N} (\sigma_j - \sigma) \left(\bar{\bar{\Gamma}}^E_{ij} \cdot \vec{E}_j\right), \quad i = 1,N \ . \tag{5.1}$$

The derivatives of $\vec{E}_i$ with respect to the conductivity of the ℓ^{th} cell can be written as

$$\frac{\partial \vec{E}_i}{\partial \sigma_\ell} = \left(\bar{\bar{\Gamma}}^E_{i\ell} \cdot \vec{E}_\ell\right) + \sum_{j=1}^{N} (\sigma_j - \sigma) \left(\bar{\bar{\Gamma}}^E_{ij} \cdot \frac{\partial \vec{E}_j}{\partial \sigma_\ell}\right), \quad \ell = 1,N \ . \tag{5.2}$$

Equation (5.2) is N linear equations for each component from which the derivatives of the electric fields in the body can be obtained. The derivatives of the surface fields with respect to the conductivities of each cell can be found by substituting $\frac{\partial \vec{E}_i}{\partial \sigma_\ell}$ into the similar equation derived from (2.14) as

$$\frac{\partial \vec{E}_k|_{z_k=0}}{\partial \sigma_\ell} = \left(\overline{\overline{\Gamma}}^E_{k\ell}|_{z_k=0} \cdot \vec{E}_\ell \right) + \sum_{j=1}^{N} (\sigma_j - \sigma) \left(\overline{\overline{\Gamma}}^E_{kj}|_{z_k=0} \cdot \frac{\partial \vec{E}_j}{\partial \sigma_\ell} \right), \quad \ell = 1,N \ . \tag{5.3}$$

Substitutions of $\vec{H}$ and $\overline{\overline{\Gamma}}^H$ into equations (5.1), (5.2), and (5.3) will produce the derivatives of the surface magnetic fields with respect to the conductivities of each cell. It is particularly interesting that for each iteration in the inversion process the same Green's functions will be used resulting in a fast iteration time.

Acknowledgements

This research has been conducted under a support by the U. S. Department of Energy through the University of California - Lawrence Berkeley Laboratory, under contract W-7405-ENG-48.

References

Erdelyi, A., et al., 1954, Tables of integral transforms: New York, McGraw-Hill.

Gradshteyn, I. S., and Ryzhik, I. M., 1965, Table of Integrals, Series, and Products: New York, Academic Press.

Harrington, R. F., 1961, Time-harmonic electromagnetic fields: New York, McGraw-Hill.

Hohmann, G. W., 1970, Electromagnetic scattering by two dimensional inhomogeneities in the earth: Berkeley, Ph.D. thesis, University of California.

Parry, J. R., 1969, Integral equation formulation of scattering from two dimensional inhomogeneities in a conductive earth: Berkeley, Ph.D. thesis, University of California.

Richmond, J. H., 1965, Scattering by a dielectric cylinder of arbitrary cross section shape: IEEE Trans., v. AP-13, p. 334-341.

Ryu, J., 1971, Low frequency electromagnetic scattering: Berkeley, Ph.D. thesis, University of California.

Somerfield, A., 1964, Partial differential equations in physics: New York, Academic Press.

Stratton, J. A., 1941, Electromagnetic theory: New York, McGraw-Hill.

Wait, J. R., 1970, Electromagnetic waves in stratified media: New York, MacMillan, 2nd edition.

(Caption of the Figures)

Figure 1.1. A two-dimensional inhomogeneity of arbitrary cross-section.

Figure 2.1. A simulation of a two-dimensional inhomogeneity by N rectangular cells.

Figure 4.1. The apparent resistivity and phase computed for the Model 1 at 100 Hertz.

Figure 4.2. The apparent resistivity and phase computed for the Model 1 at 8 Hertz.

Figure 4.3. The apparent resistivity and phase computed for the Model 2 at 100 Hertz.

Figure 4.4. The apparent resistivity and phase computed for the Model 3 at 8 Hertz.

Figure A.1. An N-layered earth with the scattering current, $\bar{J}^S$, in the ith layer.

Figure B.1. A rectangular current cell.

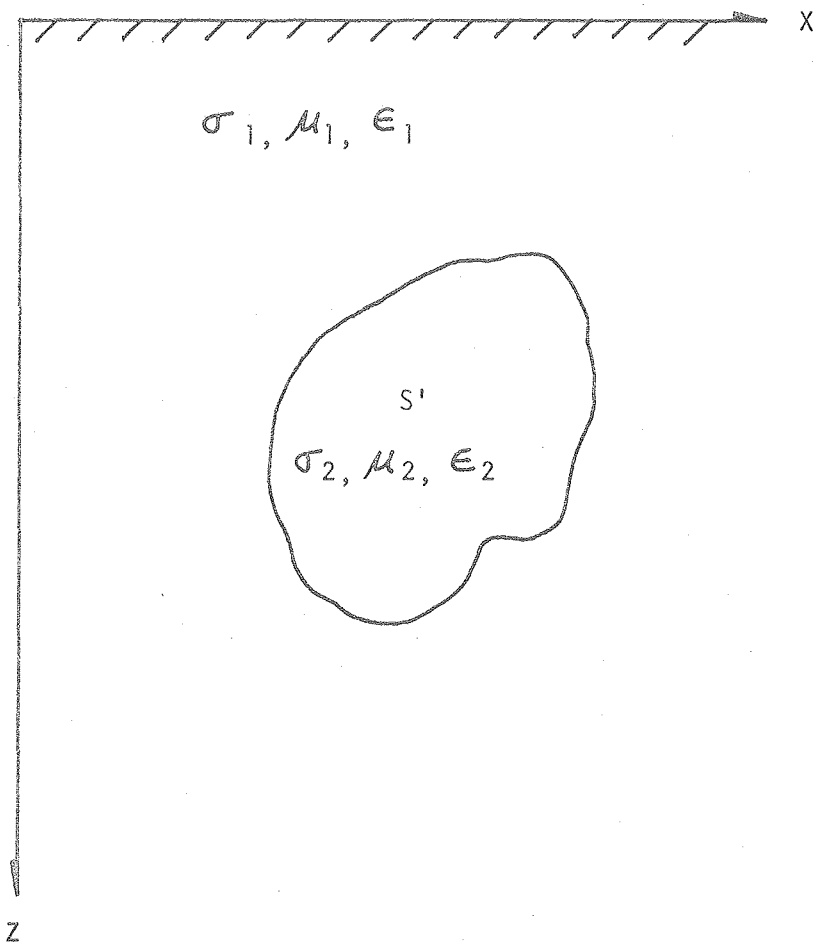

Figure 1.1

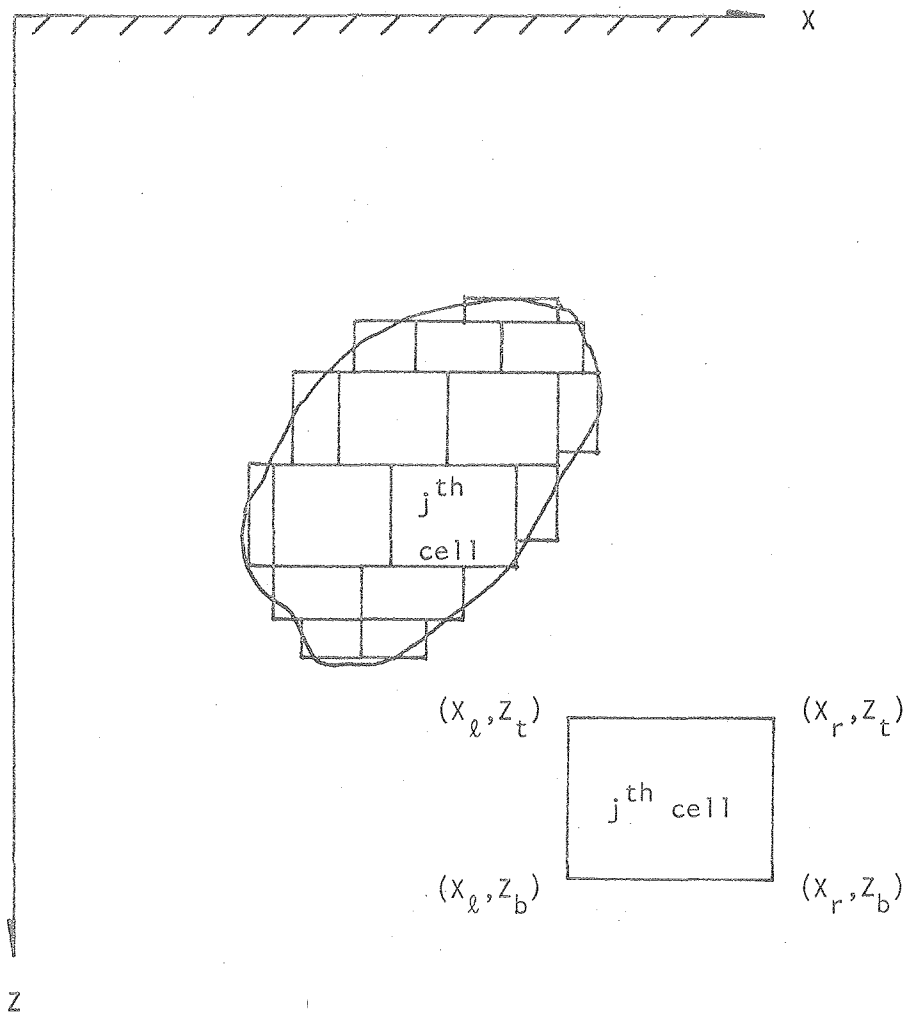

Figure 2.1

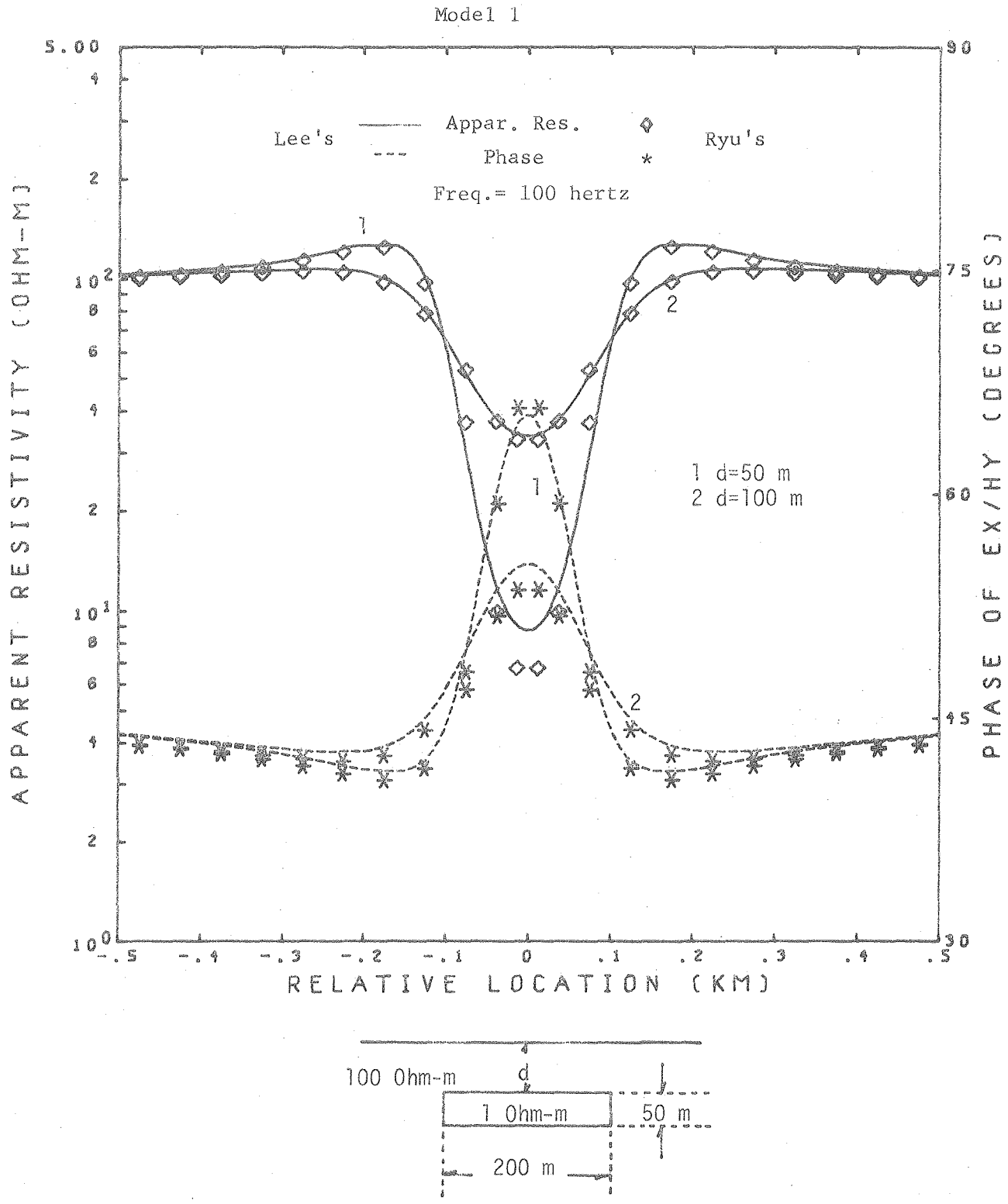
Model 1
Lee's
Appar. Res.
Phase
Ryu's
Freq.= 100 hertz
1 d=50 m
2 d=100 m
APPARENT RESISTIVITY (OHM-M)
PHASE OF EX/HY (DEGREES)
RELATIVE LOCATION (KM)
5.00
4
2
10 2
8
6
4
2
10 1
8
6
4
2
10 0
90
75
60
45
30
-.5
-.4
-.3
-.2
-.1
0
.1
.2
.3
.4
.5
100 Ohm-m
d
1 Ohm-m
50 m
200 m

Figure 4.1

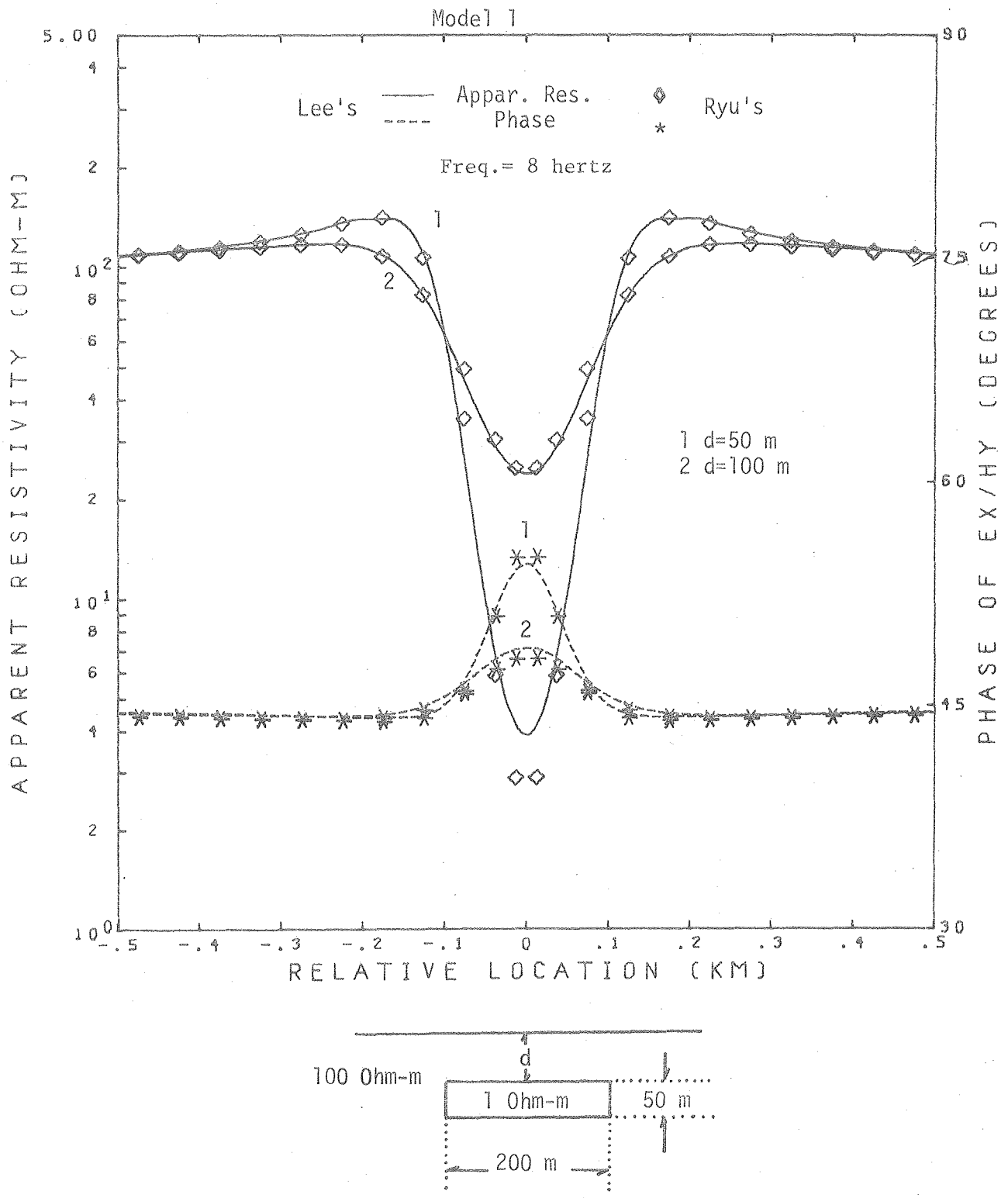
Model 1
Lee's
Appar. Res.
Phase
Ryu's
Freq.= 8 hertz
1 d=50 m
2 d=100 m
APPARENT RESISTIVITY (OHM-M)
PHASE OF EX/HY (DEGREES)
RELATIVE LOCATION (KM)
100 Ohm-m
d
1 Ohm-m
50 m
200 m

Figure 4.2

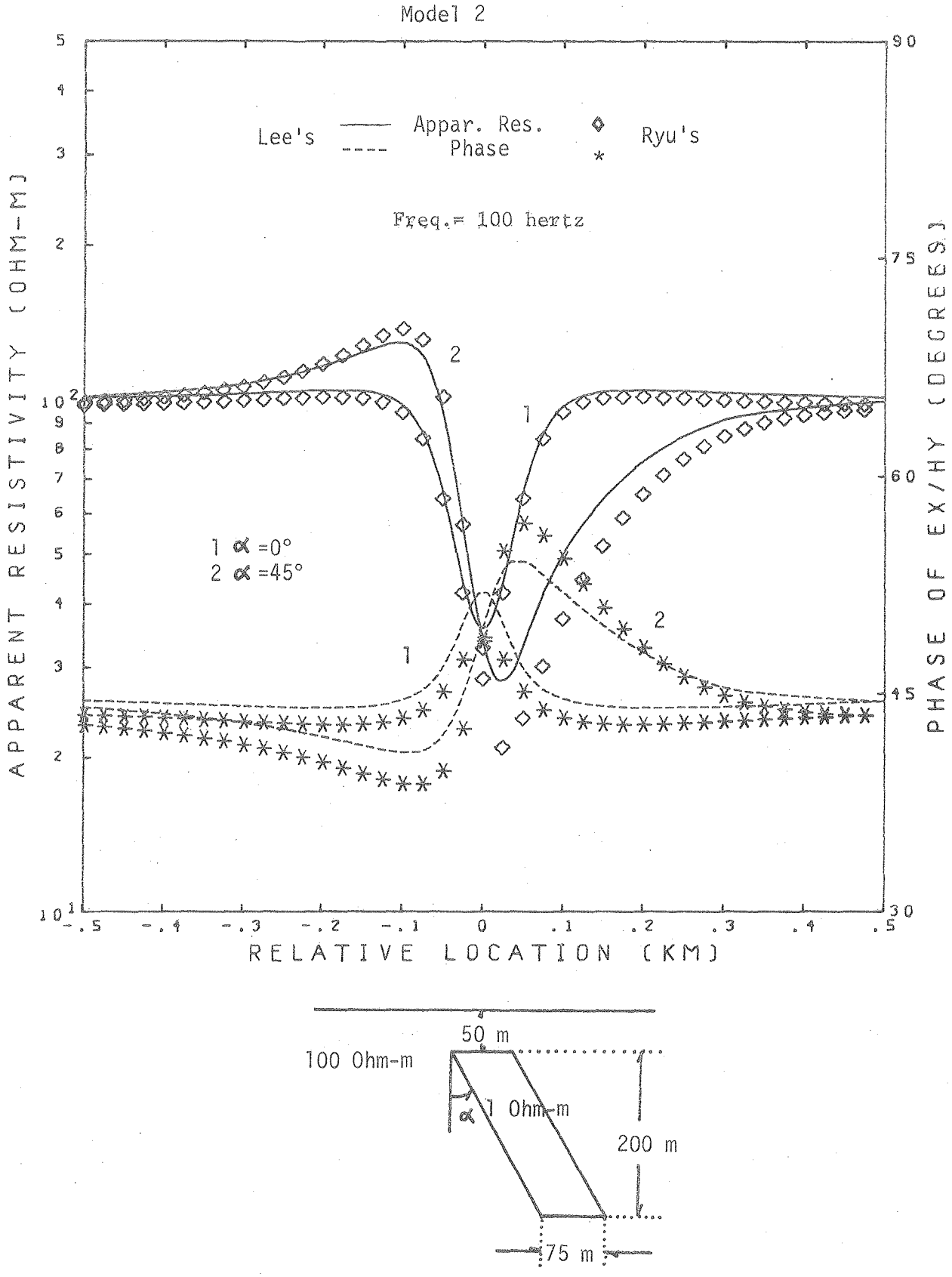
Model 2
Lee's
Appar. Res.
Phase
Ryu's
Freq.= 100 hertz
1 α =0°
2 α =45°
APPARENT RESISTIVITY (OHM-M)
PHASE OF EX/HY (DEGREES)
RELATIVE LOCATION (KM)
100 Ohm-m
50 m
1 Ohm-m
α
200 m
75 m

Figure 4.3

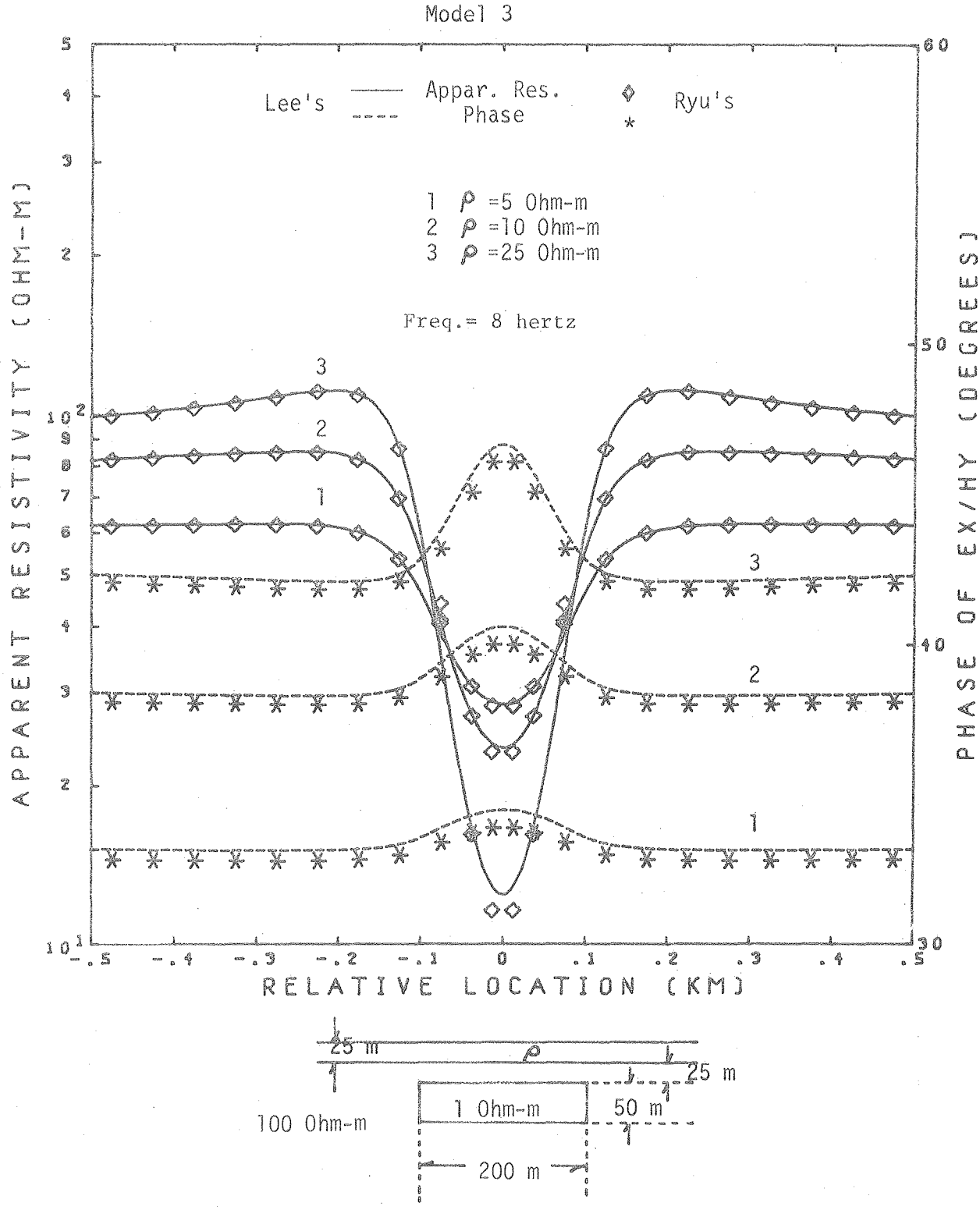
Model 3
Lee's
Appar. Res.
Phase
Ryu's
1 ρ =5 Ohm-m
2 ρ =10 Ohm-m
3 ρ =25 Ohm-m
Freq.= 8 hertz
APPARENT RESISTIVITY (OHM-M)
PHASE OF EX/HY (DEGREES)
RELATIVE LOCATION (KM)
25 m
25 m
100 Ohm-m
1 Ohm-m
50 m
200 m

Figure 4.4

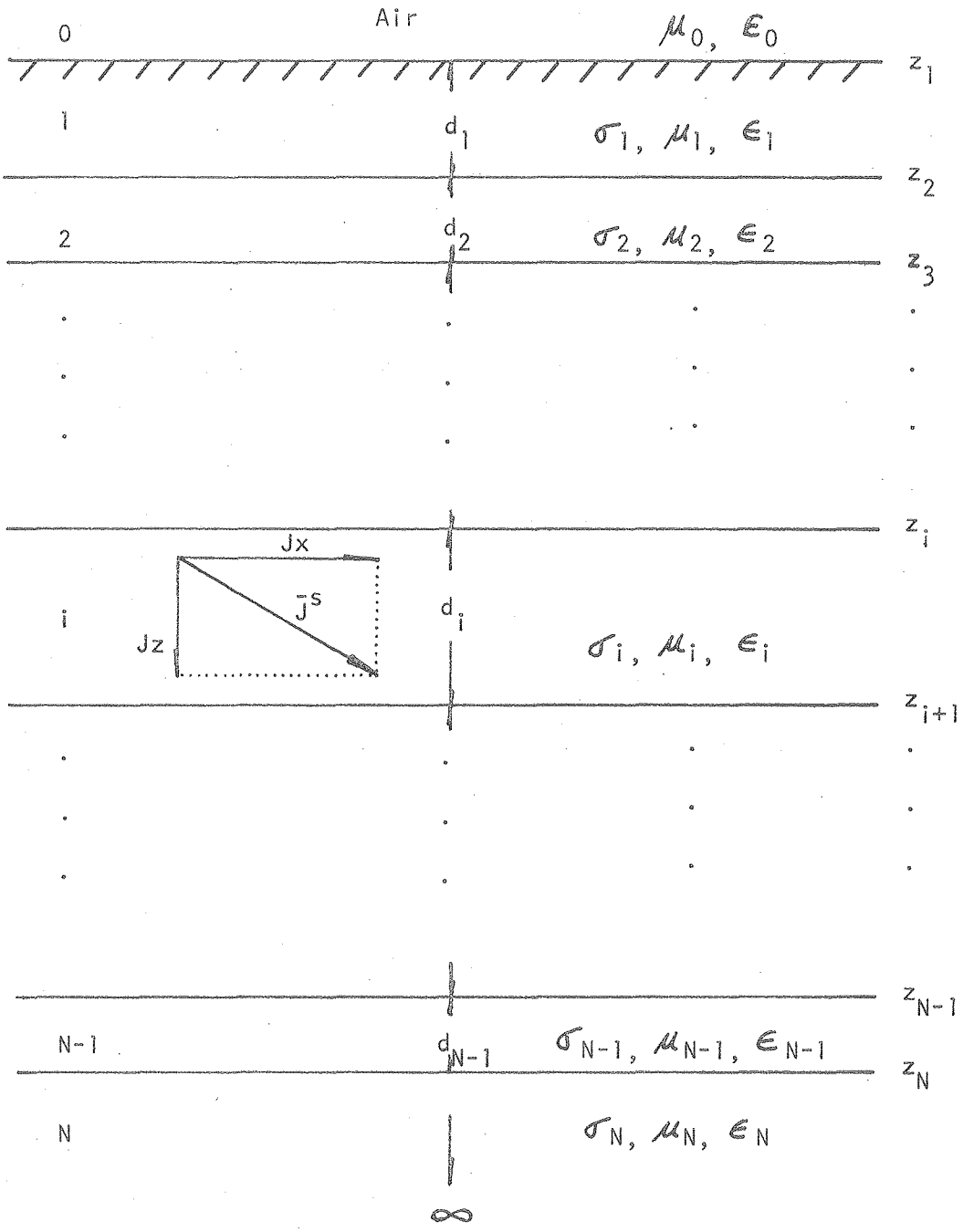
0
Air
μ_0, ϵ_0
z_1
1
d_1
$\sigma_1, \mu_1, \epsilon_1$
z_2
2
d_2
$\sigma_2, \mu_2, \epsilon_2$
z_3
z_i
Jx
$\bar{J}^s$
i
Jz
d_i
$\sigma_i, \mu_i, \epsilon_i$
z_{i+1}
z_{N-1}
N-1
d_{N-1}
$\sigma_{N-1}, \mu_{N-1}, \epsilon_{N-1}$
z_N
N
$\sigma_N, \mu_N, \epsilon_N$
∞

Figure A.1

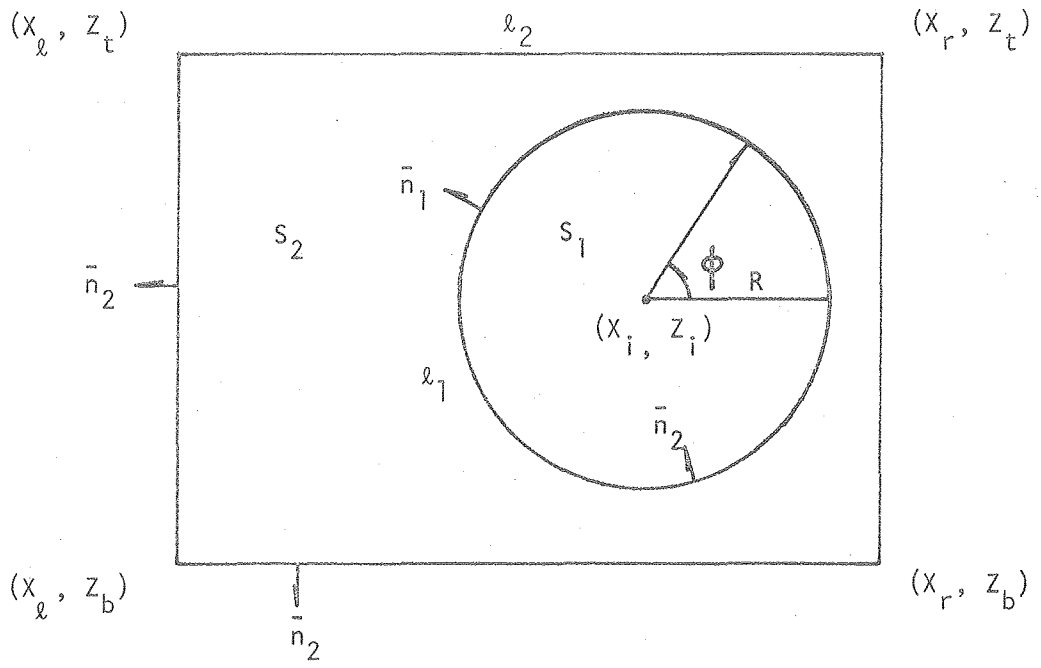
(X_ℓ, Z_t)
ℓ_2
(X_r, Z_t)
$\bar{n}_1$
S_2
S_1
$\bar{n}_2$
ϕ
R
(X_i, Z_i)
ℓ_1
$\bar{n}_2$
(X_ℓ, Z_b)
(X_r, Z_b)
$\bar{n}_2$
(X_i, Z_i)

Figure B.1

Appendix A

Consider an N-layered half space upon which a TM-mode plane wave is incident. A two-dimensional conductive inhomogeneity can be represented by a distribution of current elements over the cross sectional area oriented perpendicular to the strike. Suppose that a point current of density $\bar{J}^s$ is located at (x', z') in the i^{th} layer as shown by Figure A.1. Rewriting equation (1.17) in the i^{th} layer

$$\left(\nabla^2 + k_i^2\right) \bar{\pi}_i = - \frac{\bar{J}^s}{\sigma_i + j\omega\varepsilon_i} \delta(x - x') \, \delta(z - z') \qquad (A.1)$$

Fourier transforming (A-1), we obtain the primary potential as

$$\bar{\pi}_i^P (k_x, k_z) = - \frac{j\omega\mu}{k_i^2} \bar{J}^s \frac{e^{-j(k_x x' + k_z z')}}{u_i^2 + k_z^2} \qquad (A.2)$$

where

$$k_i^2 = (\omega^2 \mu\varepsilon_i - j\sigma_i\omega\mu)$$

$$u_i^2 = k_x^2 - k_i^2$$

$$\mu = \mu_0 = \mu_1 = \ldots = \mu_N \, .$$

Inversely transforming (A.2) in k_z (Erdelyi, 1954),

$$\bar{\pi}_i^P (k_x, z) = - \frac{j\omega\mu}{2k_i^2} \bar{J}^s e^{-jk_x x'} \frac{e^{-u_i |z - z'|}}{u_i} \, . \qquad (A.3)$$

Equation (1.19) can be rewritten in each layer as

$$\left(\nabla^2 + k_j^2\right) \bar{\pi}_j^s = 0, \qquad j = 0, N \, . \qquad (A.4)$$

The solutions for (A.4) in k_x space are written as

$$\bar{\pi}_j^s = \left[A_j(k_x) e^{-u_j z} + B_j(k_x) e^{u_j z} \right] \bar{i}_j \qquad (A.5)$$

where the directions of unit vectors $\bar{i}_j$ and the coefficients A_j and B_j are all subject to boundary conditions with initial constraints.

$$A_0(k_x) = B_N(k_x) \equiv 0 \ .$$

1. Homogeneous half space

a. $\bar{J}^s = J_x \bar{i}_x$

From (A.3) and (A.5), after dropping parentheses

$$\pi_{0x} = B_0 \, e^{u_0 z}, \qquad \text{in the air} \qquad (A.6)$$

$$\pi_{1x} = \frac{\alpha}{u_1} e^{u_1 z} + A_1 e^{-u_1 z}, \qquad \text{in the earth} \qquad (A.7)$$

where

$$\alpha = - \frac{j\omega\mu}{2k_1^2} J_x \, e^{-jk_x x'} \, e^{-u_1 z'} \ .$$

From equations (1.15) and (1.16), we have

$$E_x^s = - u^2 \pi_x \qquad (A.8)$$

$$E_z^s = - jk_x \frac{\partial \pi_x}{\partial z} \qquad (A.9)$$

$$H_y^s = - \frac{k^2}{j\omega\mu} \frac{\partial \pi_x}{\partial z} \ . \qquad (A.10)$$

Matching boundary conditions at z = 0, we obtain

$$u_0^2 B_0 = u_1^2 \left(\frac{\alpha}{u_1} + A_1\right), \qquad \text{for } E_x^s|_{z=0} \tag{A.11}$$

$$k_0^2 u_0 B_0 = k_1^2 \alpha - k_1^2 u_1 A_1, \qquad \text{for } H_y^s|_{z=0} . \tag{A.12}$$

From (A.11) and (A.12),

$$A_1 = \frac{\alpha}{u_1} R_{TM} \tag{A.13}$$

$$B_0 = 2 \frac{\alpha}{u_0} \frac{k_1^2 u_1}{k_0^2 u_1 + k_1^2 u_0} . \tag{A.14}$$

where

$$R_{TM} = - \frac{k_0^2 u_1 - k_1^2 u_0}{k_0^2 u_1 + k_1^2 u_0} .$$

Hence, the vector potential in the half space is

$$\pi_{1x} = \frac{j\omega\mu}{2\pi} \frac{J_x}{k_1^2} \int_0^\infty \frac{1}{u_1} \left[e^{-u_1|z-z'|} + R_{TM} e^{-u_1(z+z')} \right] \cos k_x(x-x') \, dk_x . \tag{A.15}$$

b. $\bar{J}^s = J_z \bar{i}_z$

In much the same way, the z-directed vector potential in the half space can be derived as

$$\pi_{1z} = -\frac{j\omega\mu}{2}\frac{J_z}{k_1^2}\int_0^\infty \frac{1}{u_1}\left[e^{-u_1|z-z'|} - R_{TM}e^{-u_1(z+z')}\right]\cos k_x(x-x')dk_x \tag{A.16}$$

2. Two-layered half space

Suppose that the inhomogeneity is in the second layer.

a. $\bar{J}^s = J_x\bar{i}_x$

The potentials in each layer can be written by using equations (A.3) and (A.5) as

$$\pi_{0x} = B_0 e^{u_0 z}, \quad \text{in the air} \tag{A.17}$$

$$\pi_{1x} = A_1 e^{-u_1 z} + B_1 e^{u_1 z}, \quad \text{in the first layer} \tag{A.18}$$

$$\pi_{2x} = \frac{\alpha}{u_2} e^{u_2 z} + A_2 e^{-u_2 z}, \quad \text{in the source region} \tag{A.19}$$

where

$$\alpha = -\frac{j\omega\mu}{2k_2^2} J_x e^{-jk_x x'} e^{-u_2 z'} .$$

Matching boundary conditions at $z = z_1$, and $z = z_2$ by substituting π_x into equations (1.15) and (1.16), we obtain at $z = z_1 = 0$,

$$B_0^2 u_0 = u_1^2 (A_1 + B_1), \quad \text{for } E_x^s\big|_{z=0} \tag{A.20}$$

$$k_0^2 u_0 B_0 = k_1^2 u_1 (-A_1 + B_1), \quad \text{for } H_y^s\big|_{z=0} \tag{A.21}$$

and at $z = z_2 = d$,

$$u_1^2 \left(A_1 e^{-u_1 d} + B_1 e^{u_1 d}\right) = u_2^2 \left(\frac{\alpha}{u_2} e^{u_2 d} + A_2 e^{-u_2 d}\right), \quad \text{for } E_x^s\big|_{z=d} \tag{A.22}$$

$$k_1^2 u_1 \left(-A_1 e^{-u_1 d} + B_1 e^{u_1 d}\right) = k_2^2 u_2 \left(\frac{\alpha}{u_2} e^{u_2 d} - A_2 e^{-u_2 d}\right), \quad \text{for } H_y^s\big|_{z=d} \tag{A.23}$$

From equations (A.20), (A.21), (A.22), and (A.23)

$$B_0 = 2\alpha \frac{k_2^2 u_2}{k_1^2 u_1} \frac{1}{u_0} {}^1R_{TM} \tag{A.24}$$

$$A_1 = \alpha \frac{k_2^2 u_2}{k_1^2 u_1} \frac{1}{u_1} \left(\frac{u_0}{u_1} - \frac{k_0^2}{k_1^2}\right) {}^1R_{TM} \tag{A.25}$$

$$B_1 = \alpha \frac{k_2^2 u_2}{k_1^2 u_1} \frac{1}{u_1} \left(\frac{u_0}{u_1} + \frac{k_0^2}{k_1^2}\right) {}^1R_{TM} \tag{A.26}$$

$$A_2 = \alpha e^{2u_2 d} \frac{1}{u_2} {}^2R_{TM} \tag{A.27}$$

where

$$ {}^{1}R_{TM} = \frac{e^{u_2 d}\ \operatorname{sech} u_1 d}{\frac{k_2^2}{k_1^2}\left(\frac{u_0}{u_1} + \frac{k_0^2}{k_1^2}\tanh u_1 d\right) + \frac{u_2}{u_1}\left(\frac{u_0}{u_1}\tanh u_1 d + \frac{k_0^2}{k_1^2}\right)} $$

$$ {}^{2}R_{TM} = \frac{\frac{k_2^2}{k_1^2}\left(\frac{u_0}{u_1} + \frac{k_0^2}{k_1^2}\tanh u_1 d\right) - \frac{u_2}{u_1}\left(\frac{u_0}{u_1}\tanh u_1 d + \frac{k_0^2}{k_1^2}\right)}{\frac{k_2^2}{k_1^2}\left(\frac{u_0}{u_1} + \frac{k_0^2}{k_1^2}\tanh u_1 d\right) + \frac{u_2}{u_1}\left(\frac{u_0}{u_1}\tanh u_1 d + \frac{k_0^2}{k_1^2}\right)} $$

The vector potentials in the first and second layers are written as

$$ \pi_{1x} = -\frac{j\omega\mu}{2\pi}\frac{J_x}{k_1^2}\int_0^\infty \frac{u_2}{u_1}\,{}^{1}R_{TM} \left[\left(\frac{u_0}{u_1} + \frac{k_0^2}{k_1^2}\right)e^{u_1 z} + \left(\frac{u_0}{u_1} - \frac{k_0^2}{k_1^2}\right)e^{-u_1 z}\right] e^{-u_2 z'} \cos k_x(x-x')\, dk_x \tag{A.28} $$

$$ \pi_{2x} = -\frac{j\omega\mu}{2\pi}\frac{J_x}{k_2^2}\int_0^\infty \frac{1}{u_2}\left[e^{-u_2|z-z'|} + {}^{2}R_{TM}\, e^{-u_2(z+z'-2d)}\right] \cdot \cos k_x(x-x')\, dk_x\ . \tag{A.29} $$

b. $\bar{J}^s = J_z \bar{i}_z$

By following similar algebraic procedures, we can easily arrive at the following vector potentials in the first and second layers.

$$ \pi_{1z} = -\frac{j\omega\mu}{2\pi}\frac{J_z}{k_1^2}\int_0^\infty \frac{1}{u_1}\,{}^{1}R_{TM} \left[\left(\frac{u_0}{u_1} + \frac{k_0^2}{k_1^2}\right)e^{u_1 z} - \left(\frac{u_0}{u_1} - \frac{k_0^2}{k_1^2}\right)e^{-u_1 z}\right] e^{-u_2 z'} \cos k_x(x-x')\, dk_x \tag{A.30} $$

$$\pi_{2z} = -\frac{j\omega\mu}{2\pi}\frac{J_z}{k_2^2}\int_0^\infty \frac{1}{u_2}\left[e^{-u_2|z-z'|} - {}^2R_{TM}\, e^{-u_2(z+z'-2d)}\right] \cdot \cos k_x(x-x')\, dk_x \tag{A.31}$$

Appendix B

The integration of the Green's function over the area occupied by the j^{th} cell of rectangular shape is evaluated at an arbitrary position (x_i, z_i).

a. Green's functions for the homogeneous half space

Rewriting equations (2.5) and (2.6), we have

$$\pi'_{1x} = \alpha \left[K_0(jk_1 r_1) + K_0(jk_1 r_2) \right] \tag{B.1}$$

$$\pi'_{1z} = \alpha \left[K_0(jk_1 r_1) - K_0(jk_1 r_2) \right] \tag{B.2}$$

where $$\alpha = - \frac{j\omega\mu}{2\pi} \frac{1}{k_1^2} .$$

Throughout the article, the following relationships are used

$$\frac{\partial}{\partial x} f(r_1) = - \frac{\partial}{\partial x'} f(r_1) \tag{B.3}$$

$$\frac{\partial}{\partial x} f(r_2) = - \frac{\partial}{\partial x'} f(r_2)$$

$$\frac{\partial}{\partial z} f(r_1) = - \frac{\partial}{\partial z'} f(r_1)$$

$$\frac{\partial}{\partial z} f(r_2) = \frac{\partial}{\partial z'} f(r_2) .$$

Figure B.1 shows the geometry of a rectangular cell in the half space. The field point (x_i, z_i) is arbitrary. If the field point is in the cell, an arbitrary circle ℓ_1 of radius R is drawn about the field point. The vectors $\bar{n}_i$, i = 1, 2, denote the unit vectors outward normal to the region

S_i, $i = 1, 2$, over which the integration is carried out.

1. $G^E_{xxij}(\bar{r};\bar{r}')$

From equations (1.22) and (B.1)

$$\Gamma^E_{xxij} = \alpha \iint_{S_j'} \left(k_1^2 + \frac{\partial^2}{\partial x^2}\right)\left[K_0(jk_1r_1) + K_0(jk_1r_2)\right] dx'dz'. \qquad (B.4)$$

If the field point is in the j^{th} cell, S_j' is divided into S_1 and S_2. The primary potential $K_0(jk_1r_1)$ is singular in S_1. The following equation holds for the vector potential $\bar{\pi}$ in the non-singular region S_2.

$$(\nabla^2 + k^2)\,\bar{\pi} = 0 \qquad (B.5)$$

By using (B.5), equation (B.4) may be rewritten

$$\begin{aligned}\Gamma^E_{xxij} = \alpha &\iint_{S_1} \left(k_1^2 + \frac{\partial^2}{\partial x^2}\right) K_0(jk_1r_1)\, ds \\ &- \alpha \iint_{S_2} \frac{\partial^2}{\partial z^2} K_0(jk_1r_1)\, ds \\ &- \alpha \iint_{S_j'} \frac{\partial^2}{\partial z^2} K_0(jk_1r_2)\, ds \qquad (B.6) \\ &= I_1 + I_2 + I_3 .\end{aligned}$$

The first part of I_1 may be evaluated in a manner similar to that used by Richmond (1965).

$$\alpha k_1^2 \iint_{S_1} K_0(jk_1r_1)\, ds = 2\pi\alpha\left[jk_1RK_1(jk_1R) - 1\right] \qquad (B.7)$$

The second part of I_1 may be evaluated in the following way: because of the symmetry,

$$\alpha \iint_{S_1} \left[\frac{\partial^2}{\partial x^2} K_0(jk_1r_1)\right]_{\bar{r}=\bar{r}_0} ds = \alpha \iint_{S_1} \left[\frac{\partial^2}{\partial z^2} K_0(jk_1r_1)\right]_{\bar{r}=\bar{r}_0} ds$$

from equation (1.17)

$$\left(\nabla^2 + k_1^2\right) \alpha k_0(jk_1r_1) = - 2\pi\alpha \, \delta(\bar{r}-\bar{r}')$$

Integration on both sides in S_1 evaluated at $\bar{r} = \bar{r}_0$ yields,

$$2\alpha \iint_{S_1} \left[\frac{\partial^2}{\partial x^2} K_0(jk_1r_1)\right]_{\bar{r}=\bar{r}_0} ds = -\alpha k_1^2 \iint_{S_1} \left[K_0(jk_1r_1)\right]_{\bar{r}=\bar{r}_0} ds$$

$$- 2\pi\alpha \iint_{S_1} \left[\delta(\bar{r}-\bar{r}')\right]_{\bar{r}=\bar{r}_0} ds$$

by (B.7)

$$= 2\pi\alpha - 2\pi\alpha \, jk_1R \, K_1(jk_1R) - 2\pi\alpha \, .$$

Hence

$$\alpha \iint_{S_1} \left[\frac{\partial^2}{\partial x^2} K_0(jk_1r_1)\right]_{\bar{r}=\bar{r}_0} ds = - jk_1\pi\alpha R \, K_1(jk_1R) \, . \qquad (B.8)$$

$$I_2 = - \alpha \iint_{S_2} \frac{\partial^2}{\partial z^2} K_0(jk_1r_1) \, ds$$

$$= - \alpha \iint_{S_2} \nabla \cdot \bar{i}_z \frac{\partial}{\partial z} K_0(jk_1r_1) \, ds$$

$$= - jk_1\alpha \int_{\ell_1} \frac{z_i - z'}{r_1} K_1(jk_1r_1) \, \bar{i}_z \cdot \bar{n}_2 \, d\ell$$

$$- jk_1\alpha \int_{\ell_2} \frac{z_i - z'}{r_1} K_1(jk_1r_1) \, \bar{i}_z \cdot \bar{n}_2 \, d\ell$$

along ℓ_2, we have

$$\bar{i}_z \cdot \bar{n}_2 = 0, \quad \text{for } x' = x_\ell, x_r$$

$$\bar{i}_z \cdot \bar{n}_2 = 1, \quad \text{for } z' = z_b$$

$$\bar{i}_z \cdot \bar{n}_2 = -1, \quad \text{for } z' = z_t,$$

hence

$$= - jk_1 \pi\alpha R \, K_1(jk_1 R)$$

$$- jk_1\alpha \int_{x_\ell}^{x_r} \left[\frac{z_i - z'}{r_1} K_1(jk_1 r_1)\right] \Big|_{z_t}^{z_b} dx' \, . \qquad (B.9)$$

Similarly,

$$I_3 = - \alpha \iint_{S_j'} \frac{\partial^2}{\partial z^2} K_0(jk_1 r_2) \, ds$$

$$= jk_1\alpha \int_{x_\ell}^{x_r} \left[\frac{z_i + z'}{r_2} K_1(jk_1 r_2)\right] \Big|_{z_t}^{z_b} dx' \, . \qquad (B.10)$$

In the case of the field point being outside of the j^{th} cell, it can be easily shown that

$$\alpha \iint_{S_j'} \left(k_1^2 + \frac{\partial^2}{\partial x^2}\right) K_0(jk_1 r_1) \, ds = - jk_1\alpha \int_{x_\ell}^{x_r} \left[\frac{z_i - z'}{r_1} K_1(jk_1 r_1)\right] \Big|_{z_t}^{z_b} dx' . \qquad (B.11)$$

Finally from equations (B.7) through (B.11)

$$\Gamma^E_{xxij} = - 2\pi\alpha \, S_{ij} - jk_1\alpha \int_{x_\ell}^{x_r} \left[\frac{z_i - z'}{r_1} K_1(jk_1 r_1) - \frac{z_i + z'}{r_2} K_1(jk_1 r_2)\right] \Big|_{z_t}^{z_b} dx' \qquad (B.12)$$

where S_{ij} is defined by

$$S_{ij} \equiv 1, \quad \text{for } x_\ell < x_i < x_r \text{ and } z_t < z_i < z_b$$

$$S_{ij} \equiv 0, \quad \text{for } (x_i, z_i) \text{ outside of } S_j' .$$

2. $G^E_{zxij}(\bar{r};\bar{r}')$

From (1.23) and (B.1)

$$\Gamma^E_{xxij} = \alpha \iint_{S_j'} \frac{\partial^2}{\partial z \partial x} \left[K_0(jk_1 r_1) + K_0(jk_1 r_2)\right] ds . \tag{B.13}$$

By (B.3)

$$\begin{aligned} \Gamma^E_{xxij} &= \alpha \iint_{S_j'} \frac{\partial^2}{\partial z' \partial x'} \left[K_0(jk_1 r_1) - K_0(jk_1 r_2)\right] ds \\ &= \alpha \left[K_0(jk_1 r_1) - K_0(jk_1 r_2)\right] \Big|_{x_\ell}^{x_r} \Big|_{z_t}^{z_b} \end{aligned} \tag{B.14}$$

3. $G^H_{yxij}(\bar{r};\bar{r}')$

From (1.24)

$$\Gamma^H_{yxij} = -\frac{\alpha k_1^2}{j\omega\mu} \iint_{S_j'} \frac{\partial}{\partial z} \left[K_0(jk_1 r_1) + K_0(jk_1 r_2)\right] ds. \tag{B.15}$$

By (B.3)

$$\begin{aligned} \Gamma^H_{yxij} &= \frac{\alpha k_1^2}{j\omega\mu} \iint_{S_j'} \frac{\partial}{\partial z'} \left[K_0(jk_1 r_1) - K_0(jk_1 r_2)\right] ds \\ &= \frac{\alpha k_1^2}{j\omega\mu} \int_{x_\ell}^{x_r} \left[K_0(jk_1 r_1) - K_0(jk_1 r_2)\right] \Big|_{z_t}^{z_b} dx' . \end{aligned} \tag{B.16}$$

4. $G^E_{xzij}(\bar{r};\bar{r}')$

From equations (1.25) and (B.2)

$$\Gamma^E_{xzij} = \alpha \iint_{S'_j} \frac{\partial^2}{\partial x \partial z} \left[K_0(jk_1r_1) - K_0(jk_1r_2)\right] ds \ . \qquad (B.17)$$

By (B.3)

$$\Gamma^E_{xzij} = \alpha \left[K_0(jk_1r_1) + K_0(jk_1r_2)\right] \Big|_{x_\ell}^{x_r} \Big|_{z_t}^{z_b} \ . \qquad (B.18)$$

5. $G_{zzij}(\bar{r};\bar{r}')$

From equation (1.26)

$$\Gamma^E_{zzij} = \alpha \iint_{S'_j} \left(k_1^2 + \frac{\partial^2}{\partial z^2}\right) \left[K_0(jk_1r_1) - K_0(jk_1r_2)\right] ds \ . \qquad (B.19)$$

As is usual, the area S_j is divided into two regions S_1 and S_2. Then by equation (B.5)

$$\Gamma^E_{zzij} = \alpha \iint_{S_1} \left(k_1^2 + \frac{\partial^2}{\partial z^2}\right) K_0(jk_1r_1)\, ds - \alpha \iint_{S_2} \frac{\partial^2}{\partial x^2} K_0(jk_1r_1)\, ds$$

$$- \alpha \iint_{S'_j} \frac{\partial^2}{\partial x^2} K_0(jk_1r_2)\, ds \ . \qquad (B.20)$$

The similar technique used for Γ^E_{xxij} yields

$$\Gamma^{E}_{zzij} = -2\pi\alpha S_{ij} - jk_1\alpha \int_{z_t}^{z_b} \left[\frac{x_i - x'}{r_1} K_1(jk_1 r_1) - \frac{x_i - x'}{r_2} K_1(jk_1 r_2) \right] \Big|_{x_\ell}^{x_r} dz' \,. \qquad (B.21)$$

6. $G^{H}_{yzij}(\bar{r};\bar{r}')$

From equation (1.27)

$$\Gamma^{H}_{yzij} = \frac{\alpha k_1^2}{j\omega\mu} \iint_{S'_j} \frac{\partial}{\partial x} \left[K_0(jk_1 r_1) - K_0(jk_1 r_2) \right] ds \,. \qquad (B.22)$$

Again by (B.3)

$$\Gamma^{H}_{yzij} = -\frac{\alpha k_1^2}{j\omega\mu} \int_{z_t}^{z_b} \left[K_0(jk_1 r_1) - K_0(jk_1 r_2) \right] \Big|_{x_\ell}^{x_r} dz' \,. \qquad (B.23)$$

b. Green's functions for the two-layered half space

1. Green's functions in the lower half space.

Rewriting π'_{2x} and π'_{2z} obtained in section 3, we have

$$\pi'_{2x} = \alpha_2 K_0(jk_2 r) + \alpha_2 \int_0^\infty \frac{1}{u_2} {}^2R_{TM} e^{-u_2(z+z')} \cos k_x(x-x') \, dk_x \tag{B.24}$$

$$\pi'_{2z} = \alpha_2 K_0(jk_2 r) - \alpha_2 \int_0^\infty \frac{1}{u_2} {}^2R_{TM} e^{-u_2(z+z')} \cos k_x(x-x') \, dk_x \tag{B.25}$$

where

$$\alpha_2 = -\frac{j\omega\mu}{2\pi} \frac{1}{k_2^2}$$

$${}^2R_{TM} = \frac{\frac{k_2^2}{k_1^2} - \frac{u_2}{u_1} \tanh u_1 d}{\frac{k_2^2}{k_1^2} + \frac{u_2}{u_1} \tanh u_1 d} e^{2u_2 d}$$

and d is the thickness of the first layer. The notation for the geometry of a rectangular cell is given in Figure B.1.

The evaluation of primary potential $K_0(jk_2 r)$ is the same as was discussed in the previous section with k_1 substituted by k_2 in the expression. By using equation (B.5) and the relationships similar to (B.3), we obtain

$$\begin{aligned} \Gamma^E_{xxij} &= \iint_{S_j} \left(k_2^2 + \frac{\partial^2}{\partial x^2}\right) \pi'_{2x} \, ds \\ &= -2\pi\alpha_2 S_{ij} - jk_2\alpha_2 \int_{x_\ell}^{x_r} \left[\frac{z_i - z'}{r} K_1(jk_2 r)\right] \Big|_{z_t}^{z_b} dx' \\ &\quad - \alpha_2 \int_0^\infty \frac{{}^2R_{TM}}{k_x} e^{-u_2 z_i} \left[e^{-u_2 z'} \sin k_x(x_i - x')\right] \Big|_{x_\ell}^{x_r} \Big|_{z_t}^{z_b} dk_x \end{aligned} \tag{B.26}$$

$$\Gamma^E_{zxij} = \iint_{S_j'} \frac{\partial^2}{\partial z \partial x} \pi'_{2x} \, ds$$

$$= \alpha_2 \, K_0(jk_2 r) \Big|_{x_\ell}^{x_r} \Big|_{z_t}^{z_b}$$

$$- \alpha_2 \int_0^\infty \frac{2R_{TM}}{u_2} e^{-u_2 z_i} \left[e^{-u_2 z'} \cos k_x (x_i - x') \right] \Big|_{x_\ell}^{x_r} \Big|_{z_t}^{z_b} dk_x \tag{B.27}$$

$$\Gamma^E_{xzij} = \iint_{S_j'} \frac{\partial^2}{\partial x \partial z} \pi'_{2z} \, ds$$

$$= \alpha_2 \, K_0(jk_2 r) \Big|_{x_\ell}^{x_r} \Big|_{z_t}^{z_b}$$

$$+ \alpha_2 \int_0^\infty \frac{2R_{TM}}{u_2} e^{-u_2 z_i} \left[e^{-u_2 z'} \cos k_x (x_i - x') \right] \Big|_{x_\ell}^{x_r} \Big|_{z_t}^{z_b} dk_x \tag{B.28}$$

$$\Gamma^E_{zzij} = \iint_{S_j'} \left(k_2^2 + \frac{\partial^2}{\partial z^2} \right) \pi'_{2z} \, ds$$

$$= -2\pi\alpha_2 \, S_{ij}$$

$$- jk_2\alpha_2 \int_{z_t}^{z_b} \left[\frac{x_i - x'}{r} K_1(jk_2 r) \right] \Big|_{x_\ell}^{x_r} dz'$$

$$- \alpha_2 \int_0^\infty \frac{k_x}{u_u^2} \, 2R_{TM} \, e^{-u_2 z_i} \left[e^{-u_2 z'} \sin k_x (x_i - x') \right] \Big|_{x_\ell}^{x_r} \Big|_{z_t}^{z_b} dk_x \, . \tag{B.29}$$

2. Green's functions on the surface.

Rewriting π'_{1x} and π'_{1z} from equations (3.5) and (3.6)

$$\pi'_{1x} = \alpha_1 \int_0^\infty {}^1R_{TM} \frac{u_2}{u_1^2} \left(e^{u_1 z} + e^{-u_1 z}\right) e^{-u_2 z'} \cos k_x(x-x')\, dk_x \tag{B.30}$$

$$\pi'_{1z} = \alpha_1 \int_0^\infty {}^1R_{TM} \frac{1}{u_1} \left(e^{u_1 z} - e^{-u_1 z}\right) e^{-u_2 z'} \cos k_x(x-x')\, dk_x \tag{B.31}$$

where

$$\alpha_1 = -\frac{j\omega\mu}{2\pi} \frac{1}{k_1^2}$$

$${}^1R_{TM} = \frac{e^{u_2 d} \operatorname{sech} u_1 d}{\frac{k_2^2}{k_1^2} + \frac{u_2}{u_1} \tanh u_1 d}.$$

Integrations of Green's functions at the k^{th} field point $(x_k, z_k = 0)$ are found to be

$$\Gamma^E_{xxkj}\Big|_{z_k=0} = -\iint_{S'_j} \frac{\partial^2}{\partial z^2} \pi'_{1x}\, ds = -2\alpha_1 \int_0^\infty \frac{{}^1R_{TM}}{k_x} \left[e^{-u_2 z'} \sin k_x(x_k - x')\right] \Big|_{x_\ell}^{x_r} \Big|_{z_t}^{z_b} dk_x \tag{B.32}$$

$$\Gamma^E_{xzkj}\Big|_{z_k=0} = \iint_{S'_j} \frac{\partial^2}{\partial x \partial z} \pi'_{1z}\, ds = 2\alpha_1 \int_0^\infty \frac{{}^1R_{TM}}{u_2} \left[e^{-u_2 z'} \cos k_x(x_k - x')\right] \Big|_{x_\ell}^{x_r} \Big|_{z_t}^{z_b} dk_x \tag{B.33}$$

$$\Gamma^{E}_{zxkj}\Big|_{z_k=0} = \Gamma^{E}_{zzkj}\Big|_{z_k=0} = 0 \qquad (B.34)$$

$$\Gamma^{H}_{yxkj}\Big|_{z_k=0} = \Gamma^{H}_{yzkj}\Big|_{z_k=0} = 0 \; . \qquad (B.35)$$

The last two results for the vertical(z) electric field and the horizontal(y) magnetic field are consistent with those concluded for the homogeneous half space case.